IEEE Access
Multidisciplinary ⋮ Rapid Review ⋮ Open Access Journal

Received March 31, 2021, accepted April 20, 2021, date of publication April 23, 2021, date of current version April 30, 2021.

Digital Object Identifier 10.1109/ACCESS.2021.3075246

Characterization of Dielectric Substrates Using Dual Band Microwave Sensor

AMMAR ARMGHAN[1], TURKI M. ALANAZI[1], AHSAN ALTAF[2], AND TANVEERUL HAQ[2], (Member, IEEE)

[1]Department of Electrical Engineering, College of Engineering, Jouf University, Sakakah 72345, Saudi Arabia
[2]INZA Research Laboratory for Electromagnetic and Microwave Engineering, Multan 60600, Pakistan

Corresponding author: Tanveerul Haq (tanveerulhaq@icloud.com)

This work was supported by the Deanship of Scientific Research at Jouf University, Al-Jouf, Saudi Arabia, under Grant 40/285.

ABSTRACT In this work, a compact, inexpensive, and efficient dual band microwave sensor is proposed. The sensor is based on two Complementary Symmetric Split-Ring Resonators (CSSRRs) and possesses a high Q factor and wide sensing range. These CSSRRs are coupled electrically with two inductive patches to the Microstrip Transmission Line (MTL). This combination provides two dual bands, first at 5.35 GHz with a notch depth of -55.20 dB and second at 7.99 GHz with a notch depth of -22.54 dB. The sensor works in transmission mode and senses shift in frequency. Some commonly available dielectric substrates with relative permittivity ranges between 1 and 12 are considered Material Under Test (MUT), and detailed sensitivity analysis is being performed for each band. The dual band sensor is fabricated on a low-cost, widely available FR4 substrate and measured by CEYEAR AV3672D vector network analyzer. Additionally, the least square curve fitting method is used to develop a mathematical model for the measured results. An excellent agreement is observed between simulated, measured, and formulated results.

INDEX TERMS Complementary symmetric split-ring resonator, dual band, microwave sensor, permittivity, high Q resonator, material under test.

I. INTRODUCTION

Material characterization technologies play a very vital role in various scientific fields [1]-[3]. These technologies find applications in the defense sector and possess a very important role in the industrial sector as well [4]. For instance, measuring structural/operational vitals of a system in an industry [5], [6] and understanding the composition of a material and/or chemical [7], [8]. These technologies also play a significant role in biomedical research [9], [10], such as neural recording [11], glucose monitoring [12], and intracranial pressure monitoring [13]. Moreover, these technologies can also locate tumors hiding within healthy tissues and muscles [14]. For these purposes, sensors based on microwaves are the best possible solutions. Several characteristics make microwave sensors standout among other available options. These attributes include low-cost [15], high sensitivity [16], label-free [17], and non-intrusive evaluation [18]. In recent years, scientists have developed microwave sensors based on metamaterials because they are very sensitive to the ambient mediums' changes in electromagnetic properties [19], [20].

In literature, many sensors are equipped with Split-Ring Resonators (SRRs) [21]-[24] and Complementary Split-Ring Resonators (CSRRs) [25]-[28]. This is because, these structures provide accuracy and high sensitivity. On the other hand, these sensors suffer from narrow bandwidth and polarization sensitiveness. To address these shortcomings, one possible solution is broadband microwave sensors. They offer the same attributes over a wide range of frequencies. Recently reported dual band sensors are based on MTL with magnetically coupled SRRs or electrically coupled CSRRs. These sensors have a sensitivity limitation due to the low Q factor and poor coupling between the MTL and the resonator [29]-[31]. In [29], a dual notch microwave sensor based on MTL and two SRRs is presented that is operating at 2.34 GHz and 2.74 GHz, and a maximum Q factor of 137 is achieved. In [30], a complementary bisymmetric split-ring resonator is coupled to MTL to operate at 4.50 GHz and 6.79 GHz, and a maximum Q factor of 145 is achieved. In [31], a dual notch microwave sensor based on MTL and two CSRRs is designed to operate at 2.22 GHz and 2.46 GHz,

The associate editor coordinating the review of this manuscript and approving it for publication was Weiren Zhu.

and a maximum Q factor of 205 is achieved. In this work, MTL was modified by introducing two inductive patches on the top plane to increase the coupling between the MTL and the resonator, and a maximum Q factor of 267.5 is achieved.

This paper presents a dual band microwave sensor comprised of two Complementary Symmetric Split-Ring Resonators (CSSRRs). The CSSRRs are a dual counterpart of the Symmetric Split-Ring Resonators (SSRRs) [32], and these resonators have been used to design waveguide bandpass filter [33] and reconfigurable stopband filter [34]. Based on the previous study [35], a low-cost and high Q sensor is proposed with mathematical modeling to evaluate common dielectric substrates. The design of the dual band sensor is elucidated in section II. Sensitivity analysis is performed in section III using thickness and permittivity perturbation techniques. Fabrication using the ultraviolet lithography technique and measurement using vector network analyzer is presented in section IV. Mathematical modeling using the least square curve fitting technique is accomplished in section V. Finally, the proposed work is concluded with technical contributions in section VI.

II. DESIGN OF DUAL BAND SENSOR

The dual band sensor is constructed on an FR4 substrate with double-sided copper cladded laminate. The relative permittivity, permeability, and dielectric loss tangent of the FR4 are 4.4, 1, and 0.02, respectively. The thickness of copper layers and substrate are 0.035 mm and 1.6 mm, respectively. The effective dielectric constant (ϵ_{re}) of the proposed transmission line is 3.326 that can be calculated using the following relation [36]:

$$\epsilon_{re} = \frac{\epsilon_r + 1}{2} + \frac{\epsilon_r - 1}{2}\left(1 + \frac{10}{u}\right)^{-ab}, \tag{1}$$

where $u = w/h$,

$$a = 1 + \frac{1}{49} ln\left(\frac{u^4 + \left(\frac{u}{52}\right)^2}{u^4 + 0.432}\right) + \frac{1}{18.7} ln\left[1 + \left(\frac{u}{18.1}\right)^3\right],$$

and

$$b = 0.564\left(\frac{\epsilon_r - 0.9}{\epsilon_r + 3}\right)^{0.053}.$$

The characteristic impedance (Z_c) of the transmission line is 50 Ω that can be calculated using the following equation [36]:

$$Z_c = \frac{\eta}{2\pi\sqrt{\epsilon_{re}}} ln\left[\frac{F}{u} + \sqrt{1 + \left(\frac{2}{u}\right)^2}\right], \tag{2}$$

where $u = w/h$, $\eta = 120\pi$ Ω, and

$$F = 6 + (2\pi - 6)\, exp\left[-\left(\frac{30.666}{u}\right)^{0.7528}\right].$$

A 3 mm wide MTL with two inductive patches is printed on the top layer of the substrate, and two Complementary Symmetric Split-Ring Resonators (CSSSRs) are etched in the bottom layer, as shown in Fig. 1. The size of the patch and CSSSRs is the same to achieve strong electromagnetic coupling. The proposed multiband sensor is simulated in ANSYS Electromagnetics Suite 2020R1 for high-performance computing with the simulation parameters and conditions given in Table 1. The magnitude of reflection (S_{11}) and transmission (S_{21}) coefficient is shown in Fig. 2. According to the simulated S_{21}, the sensor provides two notches, first at 5.37 GHz

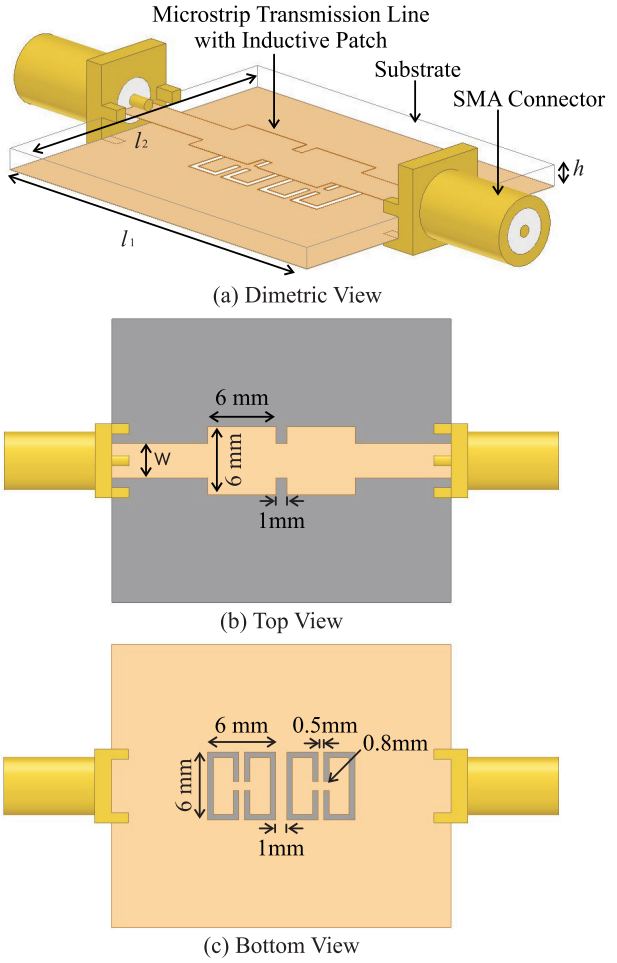

FIGURE 1. (a) Dimetric view of the proposed sensor with the dimensions: $l_1 = 30$ mm, $l_2 = 25$ mm $h = 1.6$ mm. (b) Transmission line ($w = 3$ mm) with two inductive patches. (c) Ground plane with two complementary symmetric split ring resonators.

TABLE 1. Simulation conditions for ANSYS electromagnetics suite 2020R1.

Analysis Area	Size	25x30x1.6 mm^3
	Boundary Condition	Radiation
Cells	Number	14201
	Shape	Tetrahedron
Feed		Wave port (50 Ω)
Solution Type		Driven Model
Frequency Sweep		0.1 GHz to 10 GHz
Convergence condition determination		Maximum number of passes; 20 Maximum delta S; 0.02

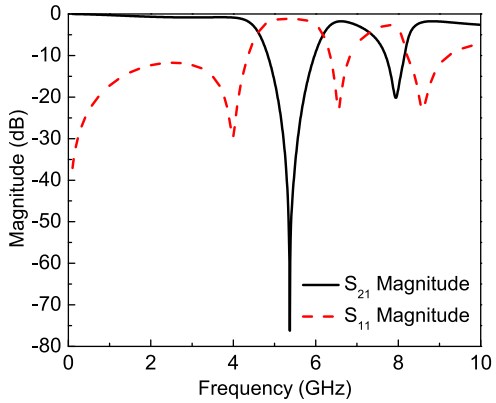

FIGURE 2. Magnitude of transmission (S_{21}) and reflection (S_{11}) coefficients. The first notch has a resonance at 5.37 GHz with a notch depth of −76.21 dB, while the second notch has a resonance at 7.95 GHz with a notch depth of −20.14 dB.

with notch depth of -76.21 dB and second at 7.95 GHz with notch depth of -20.14 dB. The S_{21} is used to calculate the unloaded Q factor of the dual notch sensor using the following relation [37]:

$$Q_{unloaded} = \frac{f_0}{f_1 - f_2}. \tag{3}$$

where, f_0 is the center resonance frequency of each notch, while f_1 is the upper and f_2 is the lower frequencies at 3 dB above the resonance. The unloaded Q factor of the first notch is 267.5, and the second notch is 53.7. The concentration of electric fields at first and second resonance is shown in Fig. 3 and Fig. 4, respectively. The maximum values of electric field at first and second resonance frequencies are 1.66×10^5 V/m and 3.74×10^5 V/m, respectively. The electric field's magnitude is high at the higher resonance frequency; therefore, the change in resonance frequency due to interaction with the MUT will be high at the second notch that will be shown in the next section.

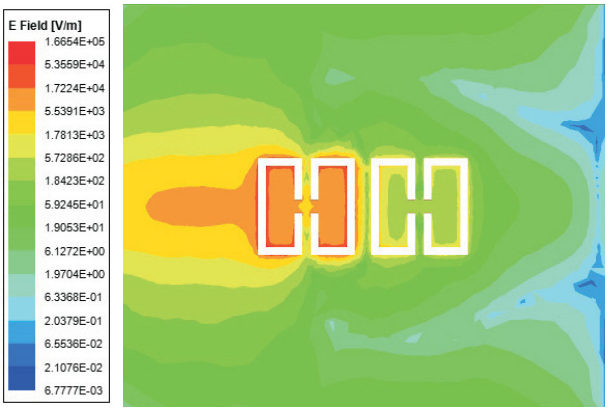

FIGURE 3. Distribution of scalar electric field in the ground plane of the proposed sensor at the first resonance.

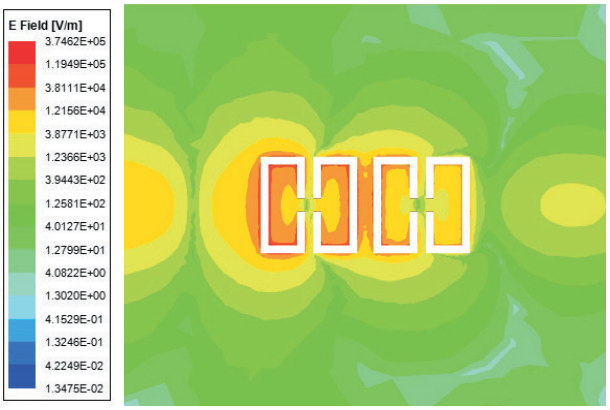

FIGURE 4. Distribution of scalar electric field in the ground plane of the proposed sensor at the second resonance.

III. SENSITIVITY ANALYSIS

To analyze the proposed sensor's sensitivity, the material under test (MUT) have to interact properly with the electromagnetic fields emitting from the CSSRRs. Therefore, MUT is placed in the sensor's ground plane with the following dimensions: $d_1 = 20$ mm, $d_2 = 15$ mm, and $d_3 = 1$ mm, as shown in Fig. 5. The fundamental principle of sensitivity in a metaresonator based microwave sensor is to observe the shift in sensor's resonance frequency with and without the MUT. When both CSSRRs are excited by the perpendicular electric fields generated by the MTL with inductive patches, it causes resonance. Without MUT, the stored electromagnetic fields (E_0 and H_0) are in an equilibrium state. When MUT is placed on the CSSRRs, it changes the capacitance of the CSSRRs and generates new electromagnetic fields (E_1 and H_1). These new electromagnetic fields shift the resonance

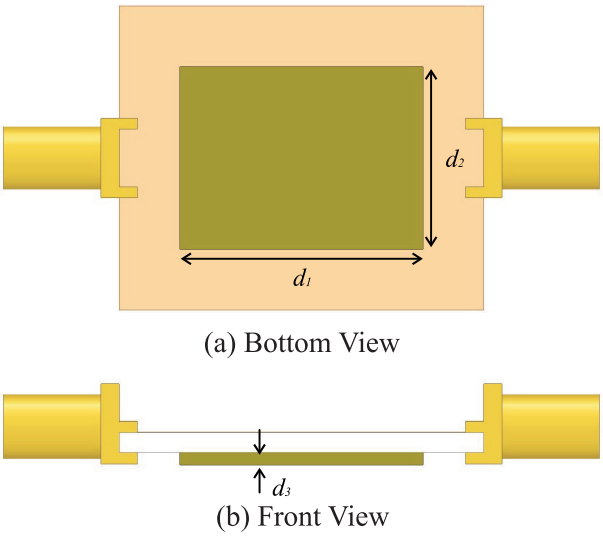

FIGURE 5. Material under test is placed in the ground plane of the proposed sensor with the following dimensions: $d_1 = 20$ mm, $d_2 = 15$ mm, and $d_3 = 1$ mm.

frequency (Δf_r) of the sensor that depends on the electromagnetic properties of the MUT, and mathematically it can be expressed as given [38]:

$$\frac{\Delta f_r}{f_r} = \frac{\int_v (\Delta\epsilon E_1.E_0 + \Delta\mu H_1.H_0)\, dv}{\int_v \left(\epsilon_0 |E_0|^2 + \mu_0 |H_0|^2\right) dv}, \tag{4}$$

According to (4), MUT's permittivity, permeability, and volume interfere with the sensor's resonance frequency. Using a volume perturbation technique, the volume of MUT (FR4) is varied by changing the height of FR4 from 0.1 mm to 1.5 mm, and its effect on the first and second notch of the proposed sensor is plotted in Fig. 6. As we increase the height of MUT, both resonance frequencies are moving towards lower values, as tabulated in Table 2. For the permittivity perturbation technique, the common available dielectric materials like HDPE ($\epsilon_r = 2.3$), PVC ($\epsilon_r = 2.7$), Rubber ($\epsilon_r = 3$), Plexiglass ($\epsilon_r = 3.4$), Polyimide-Quartz ($\epsilon_r = 4$), Glass ($\epsilon_r = 5.5$), Taconic RF-60 ($\epsilon_r = 7$), Marble ($\epsilon_r = 8.3$), Roger TMM 10 ($\epsilon_r = 9.2$), Sapphire ($\epsilon_r = 10$), and Silicon ($\epsilon_r = 11.9$), are used as MUT and their effect on the first and second band of the microwave sensor is plotted in Fig. 7 and listed in Table 3. All these MUTs are easily available in 1 mm height so the following constant dimensions: $d_1 = 20$ mm, $d_2 = 15$ mm, and $d_3 = 1$ mm are chosen for permittivity perturbation. As the relative permittivity of MUT is increased from 1.0006 to 11.9, the resonance frequency of first and second notch decreased from 5.37 GHz to 3.40 GHz and 7.95 GHz to 4.80 GHz, respectively. The sensitivity in microwave sensors based on permittivity perturbation can be defined as the ratio between the change in the sensor's resonance frequency and the change in MUT's permittivity. Mathematically sensitivity can be calculated using the following relation given [39]:

$$S = \frac{\partial f_d}{\partial \epsilon_{rd}} = \lim_{(\Delta\epsilon_{r2} - \Delta\epsilon_{r1}) \to 0} \frac{\Delta f_u - \Delta f_l}{\Delta\epsilon_{r2} - \Delta\epsilon_{r1}}. \tag{5}$$

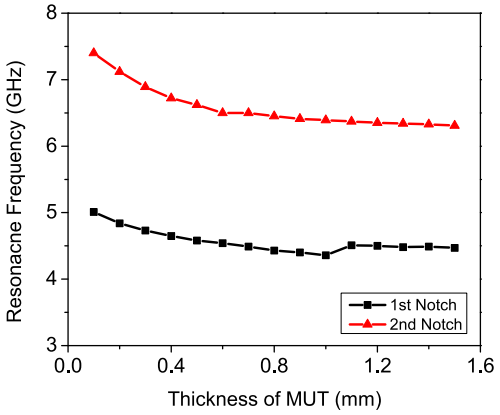

FIGURE 6. MUT's thickness versus the resonance frequency of the dual notch microwave sensor obtained by electromagnetic simulation.

Using (5), the proposed sensor's sensitivity due to the first and second resonance is extracted and plotted in Fig. 8. Two factors are crucial for sensitivity analysis. First, the shift in the sensor's resonance frequency, and the second, the permittivity of the MUT that is loaded to the sensor. According to the simulated results, it is clear that in a microwave sensor, the band with a high resonance frequency has a higher frequency shift compared to a lower one when the sensor is

TABLE 2. Effect of the MUT's thickness on the resonance frequency of the dual band microwave sensor.

Thickness of FR4 Epoxy (mm)	First Resonance Frequency (GHz)	First Notch Depth (dB)	Second Resonance Frequency (GHz)	Second Notch Depth (dB)
0.1	5.01	-53.28	7.40	-21.35
0.2	4.84	-50.72	7.12	-21.84
0.3	4.73	-48.29	6.89	-4.370
0.4	4.65	-42.70	6.72	-22.24
0.5	4.58	-40.64	6.62	-22.37
0.6	4.54	-38.20	6.50	-22.32
0.7	4.49	-36.15	6.50	-22.69
0.8	4.43	-34.28	6.45	-22.94
0.9	4.40	-32.85	6.41	-23.20
1.0	4.36	-31.86	6.39	-23.40
1.1	4.51	-30.98	6.37	-23.82
1.2	4.50	-30.31	6.35	-24.02
1.3	4.48	-29.97	6.34	-24.43
1.4	4.49	-29.42	6.33	-24.83
1.5	4.47	-29.12	6.31	-25.42

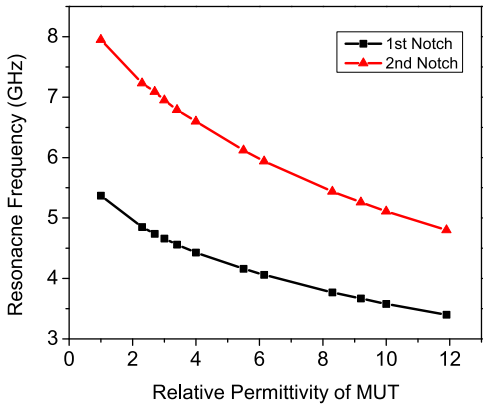

FIGURE 7. The permittivity of MUT versus the resonance frequency of the dual band microwave sensor obtained by electromagnetic simulation.

TABLE 3. Simulated transmission coefficient (S_{21}) of the dual band microwave sensor due to interaction with dielectric substrates.

Material Under Test (MUT)	Relative Permittivity	Simulated f_1 (GHz)	Notch Depth f_1 (dB)	Simulated f_2 (GHz)	Notch Depth f_2 (dB)
Air	1.0006	5.37	-76.21	7.95	-20.14
HDPE	2.3	4.85	-40.84	7.23	-24.38
PVC	2.7	4.74	-38.77	7.09	-23.96
Rubber	3	4.66	-39.17	6.95	-26.21
Plexiglass	3.4	4.56	-37.82	6.79	-26.88
Polyimide-Quartz	4	4.43	-36.62	6.60	-28.71
Glass	5.5	4.33	-34.13	6.12	-31.34
Taconic RF-60	7	4.06	-31.95	5.94	-30.30
Marble	8.3	3.77	-29.88	5.44	-34.47
Roger TMM 10	9.2	3.67	-27.98	5.26	-32.63
Sapphire	10	3.58	-28.00	5.11	-35.68
Silicon	11.9	3.40	-26.11	4.80	-34.74

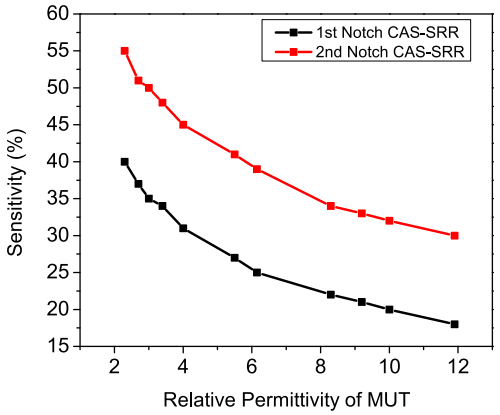

FIGURE 8. The relative permittivity of MUT versus sensitivity of the dual notch microwave sensor.

loaded with the same MUT. The other parameter is MUT's relative permittivity, which is inversely proportional to the frequency shift; therefore, as we increase the permittivity of MUT, the sensor's sensitivity starts decreasing. The first band's sensitivity lies between 18% to 40% and the second band between 30% to 55%, as listed in Table 4.

TABLE 4. The proposed sensor's sensitivity due to interaction with different MUTs.

Material Under Test (MUT)	Relative Permittivity (ϵ_r)	f_1 Sensitivity (%)	f_2 Sensitivity (%)
HDPE	2.3	40	55
PVC	2.7	37	51
Rubber	3	35	50
Plexiglass	3.4	34	48
Polyimide-Quartz	4	31	45
Glass	5.5	23	41
Taconic RF-60	7	22	34
Marble	8.3	21	34
Roger TMM 10	9.2	20	33
Sapphire	10	19	32
Silicon	11.9	18	30

IV. EXPERIMENTAL TECHNIQUE

The dual band microwave sensor is fabricated using ultraviolet (UV) lithography technique. In this technique, the proposed sensor's design is prepared in Altium Designer software to generate a Gerber file that encodes comprehensive integral information, including copper layers, resonator drawing, apertures, and other dimensions. This file is sent to the plotter after running the design for manufacture check to make a photo negative film of black ink design. After cleaning and passing through a decontamination environment, a layer of a photo-sensitive film called a photoresist is deposited on the FR4 substrate with double-sided copper cladded laminate. The sensor's design from the film is transferred to the copper layer by blasting the UV light. The photoresist is hardened on the copper layer by the UV light that passes through the film's clear parts. The unhardened photoresist is removed by washing the board with an alkaline solution to expose the unwanted copper. This exposed copper is etched by ferric trichloride solution. Meanwhile, the hardened layer of the photoresist keeps the desired copper layer protected. Finally, the hardened photoresist is removed by plasma ashing to get the desired sensor. The fabricated prototype of a dual band sensor connected with 50 Ω SMA connectors is shown in Fig. 9. The CEYEAR AV3672D series Vector Network Analyzer (VNA) is used to measure the fabricated sensor's transmission coefficient. VNA frequency characteristics like range, resolution, and accuracy are 0.01 GHz to 50 GHz, 1 Hz, and $\pm 1 \times 10^{-7}$ $(23°C \pm 3°C)$, respectively. The IF bandwidth, amplitude, and phase display resolution of VNA are 1 Hz to 5 MHz, 0.001 dB/div, and 0.01°/div, respectively. Calibration of VNA is vital to remove the uncertainties arising from the sensor's connections. Therefore, AV31123 2.4 mm kit is used to calibrate the VNA for short-circuit, open-circuit, matched load, and line calibration. After calibration, the dual notch microwave sensor's fabricated prototype is connected with the VNA, and its S_{21} is measured, as shown in Fig. 10. The comparison between the simulated and measured S_{21} is shown in Fig. 11. The simulated and measured resonance frequencies for the first band are 5.37 GHz with a notch depth of −76.21 dB and 5.35 GHz with a notch depth of −55.20 dB, respectively. The simulated and measured resonance frequencies for the second band are 7.95 GHz with a notch depth of −20.14 dB and 7.99 GHz with a notch depth of −22.54 dB, respectively. The difference between the simulated and measured resonance frequency for the first band is 0.02 GHz and the second band is 0.04 GHz, which can be attributed to the fabrication tolerance. The common available dielectric

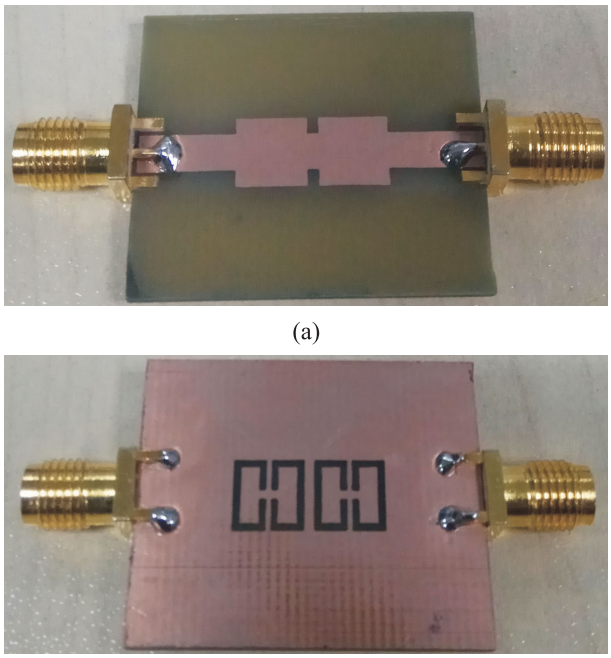

(a)

(b)

FIGURE 9. (a) Top view (b) bottom view of fabricated prototype of dual notch microwave sensor.

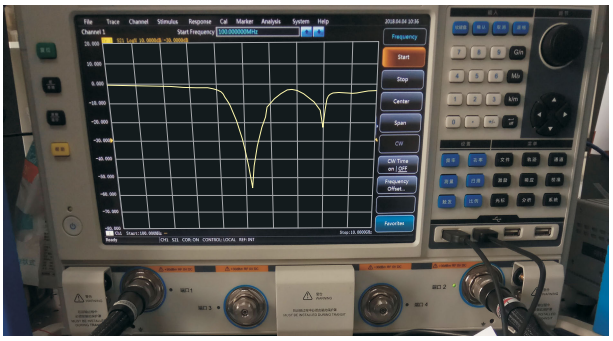

FIGURE 10. Photograph of CEYEAR AV3672D series vector network analyzer for transmission coefficient measurement of fabricated sensor.

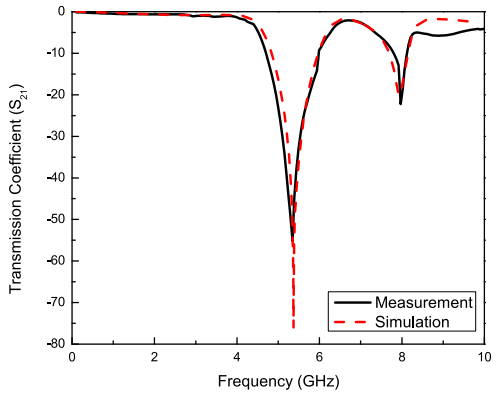

FIGURE 11. Comparison of simulated and measured transmission coefficient of the proposed sensor.

substrates with constant dimensions (20 mm × 15 mm × 1 mm) are employed on the CSSRRs in the ground plane, and the S_{21} of the dual band sensor is measured and listed in Table 5. The difference between the simulated and measured resonance frequencies due to interaction with dielectric substrate is very small, as shown in Fig. 12.

V. MATHEMATICAL MODEL OF MEASURED RESULTS

The curve fitting technique is used to construct a mathematical model. The method of least squares is used to find the best fitting curve for the measured results. For a best fitting curve, the sum of deviation must be minimum which is given as [40]:

$$\sum_{1}^{n} e_i^2 = \sum_{1}^{n} [y_i - f\,(x_i)]^2 \tag{6}$$

where x is the independent variable and y is the dependent variable and e_i is the deviation (error). For the best fitting polynomial $y = a + bx + cx^2$ the least error (E) is:

$$E = \sum_{1}^{n} e_i^2 = \sum_{1}^{n} \left[y_i - \left(a + bx_i + cx_i^2\right)\right]^2 \tag{7}$$

$\frac{\partial E}{\partial a} = 0$, $\frac{\partial E}{\partial b} = 0$, and $\frac{\partial E}{\partial c} = 0$ are the conditions for least error to be minimum. Using these conditions the following matrix is formulated to find the unknown coefficients

TABLE 5. Measured transmission coefficient (S_{21}) of the dual band microwave sensor due to interaction with dielectric substrates.

Material Under Test (MUT)	Relative Permittivity	Measured f_1 (GHz)	Notch Depth f_1 (dB)	Measured f_2 (GHz)	Notch Depth f_2 (dB)
Air	1.0006	5.35	-55.20	7.99	-22.54
HDPE	2.3	4.92	-35.74	7.26	-25.48
PVC	2.7	4.73	-33.67	7.11	-25.86
Rubber	3	4.65	-32.17	6.98	-27.31
Plexiglass	3.4	4.55	-31.82	6.83	-27.78
Polyimide-Quartz	4	4.40	-30.62	6.64	-29.61
Glass	5.5	4.08	-30.13	6.15	-32.54
Taconic RF-60	6.15	4.01	-29.95	6.01	-31.40
Marble	8.3	3.71	-28.88	5.47	-35.57
Roger TMM 10	9.2	3.64	-25.98	5.29	-33.73
Sapphire	10	3.53	-24.00	5.15	-36.78
Silicon	11.9	3.37	-23.11	4.86	-35.64

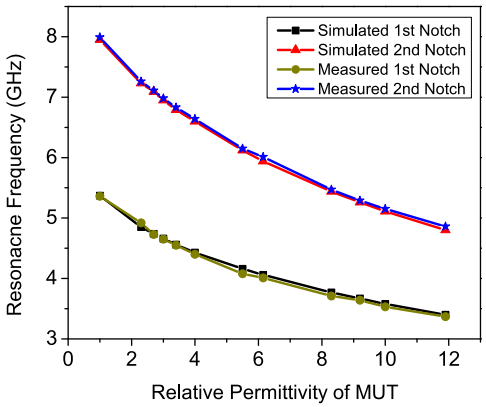

FIGURE 12. The difference between the simulated and measured resonance frequencies due to interaction with dielectric substrate.

TABLE 6. Comparison of simulated, measured and formulated results for the first resonance frequency of the sensor due to interaction with different MUTs.

Material Under Test (MUT)	Relative Permittivity	Simulated f_1 (GHz)	Measured f_1 (GHz)	Formulated f_1 (GHz)
Air	1.0006	5.37	5.35	5.28
HDPE	2.3	4.85	4.92	4.88
PVC	2.7	4.74	4.73	4.77
Rubber	3	4.66	4.65	4.69
Plexiglass	3.4	4.56	4.55	4.58
Polyimide-Quartz	4	4.43	4.40	4.43
Glass	5.5	4.16	4.08	4.10
Taconic RF-60	6.15	4.06	4.01	3.97
Marble	8.3	3.77	3.71	3.64
Roger TMM 10	9.2	3.67	3.64	3.54
Sapphire	10	3.58	3.53	3.48
Silicon	11.9	3.40	3.37	3.38

(a, b, and c) of the polynomial:

$$\begin{bmatrix} a \\ b \\ c \end{bmatrix} = \begin{bmatrix} n & \sum x_i & \sum x_i^2 \\ \sum x_i & \sum x_i^2 & \sum x_i^3 \\ \sum x_i^2 & \sum x_i^3 & \sum x_i^4 \end{bmatrix}^{-1} \begin{bmatrix} \sum y_i \\ \sum x_i y_i \\ \sum x_i^2 y_i \end{bmatrix} \tag{8}$$

In our case, ϵ_r is independent variable and f is dependent variable which can be expressed by the following polynomial:

$$f_i = a + b\epsilon_r + c\epsilon_r^2 \tag{9}$$

TABLE 7. Comparison of simulated, measured and formulated results for second resonance frequency of the sensor due to interaction with different MUTs.

Material Under Test (MUT)	Relative Permittivity	Simulated f_2 (GHz)	Measured f_2 (GHz)	Formulated f_2 (GHz)
Air	1.0006	7.95	7.99	7.87
HDPE	2.3	7.23	7.26	7.30
PVC	2.7	7.09	7.11	7.14
Rubber	3	6.95	6.98	7.02
Plexiglass	3.4	6.79	6.83	6.86
Polyimide-Quartz	4	6.60	6.64	6.64
Glass	5.5	6.12	6.15	6.14
Taconic RF-60	6.15	5.94	6.01	5.95
Marble	8.3	5.44	5.47	5.41
Roger TMM 10	9.2	5.26	5.29	5.23
Sapphire	10	5.11	5.15	5.09
Silicon	11.9	4.80	4.86	4.86

TABLE 8. Comparison of various state of art sensors based on different type of resonators.

Ref.	Resonator Type	Fundamental Resonance f_0 (GHz)	$S_{Av.}$ (MHz)	$S_{Av.,f}$ (%)	Size
[41]	SSRR	2.4	13.4	0.5	N.G.
[42]	SRRs	0.87	0.79	0.91	$0.1\lambda_g^2$
[43]	SIRs	3	54.3	1.81	$0.046\lambda_g^2$
[44]	CSRRs	1.7	33.3	1.96	$0.098\lambda_g^2$
[45]	SRRs	2.1	72	3.4	$0.034\lambda_g^2$
[46]	LC Resonator	2.41	90	3.73	N.G.
[47]	Magnetic LC Resonator	2.18	88	4.03	$0.02\lambda_g^2$
[48]	SIRs	6.1	536	8.8	$0.15\lambda_g^2$
Proposed	CSSRRs	5.35	520	9.7	$0.23\lambda_g^2$

For f_1 and f_2 of the fabricated sensor, the unknown coefficients (a, b, and c) are calculated using matrix (8) and measured data given in Table 5. The mathematical models for first and second resonance are given as:

$$f_1 = 5.630 - 0.355\epsilon_r + 0.014\epsilon_r^2 \quad (10)$$

$$f_2 = 8.359 - 0.496\epsilon_r + 0.017\epsilon_r^2 \quad (11)$$

Comparison of simulated, measured, and formulated results of the proposed sensor for first and second resonance frequencies are tabulated in Table 6 and Table 7, respectively. A satisfactory agreement is achieved between the simulated, measured and formulated results. The proposed sensor is compared with other state of the art sensors for average sensitivity ($S_{Av.}$), normalized average sensitivity ($S_{Av.,f}$), and size. The performance of presented sensor in term of $S_{Av.,f}$ is high as compared to other sensors as listed in Table 8.

VI. CONCLUSION

In this work, a novel microwave sensor is designed and simulated using a full-wave electromagnetic software ANSYS Electromagnetics Suite 2020R1, fabricated using ultraviolet (UV) lithography technique, and measured by CEYEAR AV3672D vector network analyzer. Furthermore, least square curve fitting technique is used to obtain mathematical model of the system and an excellent agreement is observed between simulated and experimental results. The proposed design is based on two complementary symmetric split-ring resonators (CSSRRs) that are electrically coupled to the microstrip transmission line using two inductive patches. To extract the permittivity of material under test, dual band response is utilized. The Q factor of first and second resonances are 267.5 and 53.7, respectively. Due to high Q factor and wide sensing range, this sensor can be used to characterize various commonly available dielectric substrates. The sensitivity of the first and second resonance of the dual notch sensor due to interaction with the HDPE substrate is 40% and 55%, respectively. A brief comparison of the proposed work with the available works reported in the literature is also presented and it is observed that the normalized average sensitivity of the proposed sensor is greater than the other available sensors. It is worthy to note that the proposed dual notch sensor has a miniaturized and compact size, and it is fabricated using a simple and an inexpensive technique.

REFERENCES

[1] A. P. Viswanathan, R. Moolat, M. Mani, S. Va, and M. Pezholil, "A simple electrically small microwave sensor based on complementary asymmetric single split resonator for dielectric characterization of solids and liquids," *Int. J. RF Microw. Comput.-Aided Eng.*, vol. 30, no. 12, pp. 1–13, Oct. 2020.

[2] T. Haq, C. Ruan, X. Zhang, S. Ullah, A. K. Fahad, and W. He, "Extremely sensitive microwave sensor for evaluation of dielectric characteristics of low-permittivity materials," *Sensors*, vol. 20, pp. 1–17, Mar. 2020.

[3] P. Vélez, K. Grenier, J. Mata-Contreras, D. Dubuc, and F. Martin, "Highly-sensitive microwave sensors based on open complementary split ring resonators (OCSRRs) for dielectric characterization and solute concentration measurement in liquids," *IEEE Access*, vol. 6, pp. 48324–48338, Sep. 2018.

[4] D. Prakash and N. Gupta, "Applications of metamaterial sensors: A review," *Int. J. Microw. Wireless Technol.*, pp. 1–5, Feb. 2021.

[5] A. K. Jha, N. Delmonte, A. Lamecki, M. Mrozowski, and M. Bozzi, "Novel MNZ-type microwave sensor for testing magnetodielectric materials," *Sci. Rep.*, vol. 10, no. 1, pp. 1–13, Oct. 2020.

[6] L.-C. Fan, W.-S. Zhao, H.-Y. Gan, L. He, Q. Liu, L. Dong, and G. Wang, "A high-Q active substrate integrated waveguide based sensor for fully characterizing magneto-dielectric (MD) materials," *Sens. Actuators A, Phys.*, vol. 301, pp. 1–26, Jan. 2020.

[7] A. P. Saghati, J. S. Batra, J. Kameoka, and K. Entesari, "A metamaterial-inspired wideband microwave interferometry sensor for dielectric spectroscopy of liquid chemicals," *IEEE Trans. Microw. Theory Techn.*, vol. 65, no. 7, pp. 2558–2571, Jul. 2017.

[8] A. Ebrahimi, F. J. Tovar-Lopez, J. Scott, and K. Ghorbani, "Differential microwave sensor for characterization of glycerol-water solutions," *Sens. Actuators B, Chem.*, vol. 321, no. 10, pp. 1–8, Oct. 2020.

[9] H.-J. Lee, J.-H. Lee, H.-S. Moon, I.-S. Jang, J.-S. Choi, J.-G. Yook, and H.-I. Jung, "A planar split-ring resonator-based microwave biosensor for label-free detection of biomolecules," *Sens. Actuators B, Chem.*, vol. 169, pp. 26–31, Jul. 2012.

[10] S. RoyChoudhury, V. Rawat, A. H. Jalal, S. N. Kale, and S. Bhansali, "Recent advances in metamaterial split-ring-resonator circuits as biosensors and therapeutic agents," *Biosensors Bioelectron.*, vol. 86, pp. 595–608, Dec. 2016.

[11] A. Sharma, E. Kampianakis, and M. S. Reynolds, "A dual-band HF and UHF antenna system for implanted neural recording and stimulation devices," *IEEE Antennas Wireless Propag. Lett.*, vol. 16, pp. 493–496, Jun. 2017.

[12] L. W. Liu, A. Kandwal, Q. Cheng, H. Shi, I. Tobore, and Z. Nie, "Non-invasive blood glucose monitoring using a curved Goubau line," *Electronics*, vol. 8, no. 6, pp. 1–12, Jun. 2019.

[13] S. A. A. Shah and H. Yoo, "Scalp-implantable antenna systems for intracranial pressure monitoring," *IEEE Trans. Antennas Propag.*, vol. 66, no. 4, pp. 2170–2173, Apr. 2018.

[14] M. A. Aldhaeebi, K. Alzoubi, T. S. Almoneef, S. M. Bamatraf, H. Attia, and O. M. Ramahi, "Review of microwaves techniques for breast cancer detection," *Sensors*, vol. 20, no. 8, pp. 1–38, Apr. 2020.
[15] A. E. Omer, G. Shaker, S. Safavi-Naeini, H. Kokabi, G. Alquié, F. Deshours, and R. M. Shubair, "Low-cost portable microwave sensor for non-invasive monitoring of blood glucose level: Novel design utilizing a four-cell CSRR hexagonal configuration," *Sci. Rep.*, vol. 10, no. 1, pp. 1–20, Sep. 2020.
[16] X. Zhang, C. Ruan, T. Haq, and K. Chen, "High-sensitivity microwave sensor for liquid characterization using a complementary circular spiral resonator," *Sensors*, vol. 19, no. 4, pp. 1–14, Feb. 2019.
[17] R. Kumari, P. N. Patel, and R. Yadav, "An ENG-inspired microwave sensor and functional technique for label-free detection of Aspergillus Niger," *IEEE Sensors J.*, vol. 18, no. 10, pp. 3932–3939, May 2018.
[18] M. H. Zarifi, H. Sadabadi, S. H. Hejazi, M. Daneshmand, and A. Sanati-Nezhad, "Noncontact and nonintrusive microwave-microfluidic flow sensor for energy and biomedical engineering," *Sci. Rep.*, vol. 8, no. 1, pp. 1–10, Jan. 2018.
[19] T. Haq, C. Ruan, X. Zhang, and S. Ullah, "Complementary metamaterial sensor for nondestructive evaluation of dielectric substrates," *Sensors*, vol. 19, no. 9, pp. 1–13, May 2019.
[20] A. Ebrahimi, J. Scott, and K. Ghorbani, "Ultrahigh-sensitivity microwave sensor for microfluidic complex permittivity measurement," *IEEE Trans. Microw. Theory Techn.*, vol. 67, no. 10, pp. 4269–4277, Oct. 2019.
[21] M. Abdolrazzaghi, S. Khan, and M. Daneshmand, "A dual-mode split-ring resonator to eliminate relative humidity impact," *IEEE Microw. Wireless Compon. Lett.*, vol. 28, no. 10, pp. 939–941, Oct. 2018.
[22] J. Mata-Contreras, C. Herrojo, and F. Martín, "Application of split ring resonator (SRR) loaded transmission lines to the design of angular displacement and velocity sensors for space applications," *IEEE Trans. Microw. Theory Techn.*, vol. 65, no. 11, pp. 4450–4460, Nov. 2017.
[23] M. G. Mayani, F. J. Herraiz-Martínez, J. M. Domingo, and R. Giannetti, "Resonator-based microwave metamaterial sensors for instrumentation: Survey, classification, and performance comparison," *IEEE Trans. Instrum. Meas.*, vol. 70, pp. 1–14, Nov. 2021.
[24] A. A. M. Bahar, Z. Zakaria, S. R. A. Rashid, A. A. M. Isa, and R. A. Alahnomi, "High-efficiency microwave planar resonator sensor based on bridge split ring topology," *IEEE Microw. Wireless Compon. Lett.*, vol. 27, no. 6, pp. 545–547, Jun. 2017.
[25] E. L. Chuma, Y. Iano, G. Fontgalland, and L. L. B. Roger, "Microwave sensor for liquid dielectric characterization based on metamaterial complementary split ring resonator," *IEEE Sensors J.*, vol. 18, no. 24, pp. 9978–9983, Dec. 2018.
[26] M. Saadat-Safa, V. Nayyeri, M. Khanjarian, M. Soleimani, and O. M. Ramahi, "A CSRR-based sensor for full characterization of magneto-dielectric materials," *IEEE Trans. Microw. Theory Techn.*, vol. 67, no. 2, pp. 806–814, Feb. 2019.
[27] H.-Y. Gan, W.-S. Zhao, L. He, Y. Yu, K. Xu, F. Wen, L. Dong, and G. Wang, "A CSRR-loaded planar sensor for simultaneously measuring permittivity and permeability," *IEEE Microw. Wireless Compon. Lett.*, vol. 30, no. 2, pp. 219–221, Feb. 2020.
[28] S. A. Alotaibi, Y. Cui, and M. M. Tentzeris, "CSRR based sensors for relative permittivity measurement with improved and uniform sensitivity throughout [0.9–10.9] GHz band," *IEEE Sensors J.*, vol. 20, no. 9, pp. 4667–4678, May 2020.
[29] S. K. T. Muhammed, M. A. H. Ansari, A. K. Jha, and M. J. Akhtar, "Design of SRR-based microwave sensor for characterization of magnetodielectric substrates," *IEEE Microw. Wireless Compon. Lett.*, vol. 27, no. 5, pp. 524–526, May 2017.
[30] T. Haq, C. Ruan, S. Ullah, and A. K. Fahad, "Dual notch microwave sensors based on complementary metamaterial resonators," *IEEE Access*, vol. 7, pp. 153489–153498, Nov. 2019.
[31] W.-S. Zhao, H.-Y. Gan, L. He, Q. Liu, D.-W. Wang, K. Xu, S. Chen, L. Dong, and G. Wang, "Microwave planar sensors for fully characterizing magneto-dielectric materials," *IEEE Sensors J.*, vol. 20, no. 19, pp. 11326–11334, Oct. 2020.
[32] S. Brien and J. B. Pendry, "Magnetic activity at infrared frequencies in structured metallic photonic crystals," *J. Phys., Condens. Matter*, vol. 14, pp. 6383–6394, Jun. 2002.
[33] T. U. Haq, M. F. Khan, and O. F. Siddiqui, "Design and implementation of waveguide bandpass filter using complementary metaresonator," *Appl. Phys. A, Solids Surf.*, vol. 122, no. 1, pp. 1–5, Dec. 2015.
[34] T. U. Haq, C. Ruan, S. Ullah, and A. Kosar, "Reconfigurable ultra wide band notch filter based on complementary metamaterial," in *Proc. IEEE Asia–Pacific Conf. Antennas Propag. (APCAP)*, Auckland, New Zealand, Aug. 2018, pp. 381–382.
[35] T. Ul Haq, C. Ruan, R. Wang, and T. Wu, "High Q dual band super high frequency notch filter based on complementary metamaterial," in *Proc. Prog. Electromagn. Res. Symp. (PIERS)*, Toyama, Japan, Aug. 2018, pp. 1254–1257.
[36] J. S. Hong, *Microstrip Filters for RF/Microwave Applications*. Hoboken, NJ, USA: Wiley, 2011, pp. 77–78.
[37] T. Haq, C. Ruan, X. Zhang, A. Kosar, and S. Ullah, "Low cost and compact wideband microwave notch filter based on miniaturized complementary metaresonator," *Appl. Phys. A, Solids Surf.*, vol. 125, no. 9, pp. 1–7, Aug. 2019.
[38] D. M. Pozer, *Microwave Engineering*. Hoboken, NJ, USA: Wiley, 2012, pp. 306–308.
[39] S. A. Qureshi, Z. Z. Abidin, A. Y. I. Ashyap, H. A. Majid, M. R. Kamarudin, M. Yue, M. S. Zulkipli, and J. Nebhen, "Millimetre-wave metamaterial-based sensor for characterisation of cooking oils," *Int. J. Antennas Propag.*, vol. 2021, pp. 1–10, Mar. 2021.
[40] K. Molugaram and G. S. Rao, *Statistical Techniques for Transportation Engineering*. Amsterdam, The Netherlands: Elsevier, 2017, pp. 281–283.
[41] M. H. Zarifi and M. Daneshmand, "Wide dynamic range microwave planar coupled ring resonator for sensing applications," *Appl. Phys. Lett.*, vol. 108, no. 23, Jun. 2016, Art. no. 232906.
[42] P. Vélez, L. Su, K. Grenier, J. Mata-Contreras, D. Dubuc, and F. Martín, "Microwave microfluidic sensor based on a microstrip splitter/combiner configuration and split ring resonators (SRRs) for dielectric characterization of liquids," *IEEE Sensors J.*, vol. 17, no. 20, pp. 6589–6598, Oct. 2017.
[43] L. Su, J. Mata-Contreras, P. Vélez, and F. Martín, "Configurations of splitter/combiner microstrip sections loaded with stepped impedance resonators (SIRs) for sensing applications," *Sensors*, vol. 16, no. 12, p. 2195, Dec. 2016.
[44] L. Su, J. Mata-Contreras, P. Velez, and F. Martin, "Splitter/combiner microstrip sections loaded with pairs of complementary split ring resonators (CSRRs): Modeling and optimization for differential sensing applications," *IEEE Trans. Microw. Theory Techn.*, vol. 64, no. 12, pp. 4362–4370, Dec. 2016.
[45] A. Ebrahimi, J. Scott, and K. Ghorbani, "Differential sensors using microstrip lines loaded with two split-ring resonators," *IEEE Sensors J.*, vol. 18, no. 14, pp. 5786–5793, Jul. 2018.
[46] A. Ebrahimi, J. Scott, and K. Ghorbani, "Transmission lines terminated with LC resonators for differential permittivity sensing," *IEEE Microw. Wireless Compon. Lett.*, vol. 28, no. 12, pp. 1149–1151, Dec. 2018.
[47] A. Ebrahimi, G. Beziuk, J. Scott, and K. Ghorbani, "Microwave differential frequency splitting sensor using magnetic-LC resonators," *Sensors*, vol. 20, no. 4, p. 1066, Feb. 2020.
[48] J. Naqui, C. Damm, A. Wiens, R. Jakoby, L. Su, J. Mata-Contreras, and F. Martin, "Transmission lines loaded with pairs of stepped impedance resonators: Modeling and application to differential permittivity measurements," *IEEE Trans. Microw. Theory Techn.*, vol. 64, no. 11, pp. 3864–3877, Nov. 2016.

AMMAR ARMGHAN was born in Faisalabad, Pakistan, in February 1984. He received the B.S. degree in electrical engineering from COMSATS University Islamabad, in 2006, the M.S. degree in electronics and communication engineering from the University of Nottingham, in 2010, and the Ph.D. degree from the Wuhan National Laboratory of Optoelectronics, Huazhong University of Science and Technology, Wuhan, China, in 2016. In 2006, he joined the School of Electrical Engineering, The University of Faisalabad, as a Lecturer. He is currently working as an Assistant Professor. His research interest includes complementary metamaterial based microwave and terahertz devices.

TURKI M. ALANAZI received the B.Sc. degree (Hons.) from the Bluefield State College, Bluefield, WV, USA, in 2010, the M.Sc. degree from Gannon University, Erie, PA, USA, in 2011, and the Ph.D. degree from the University of Dayton, Dayton, OH, USA, in 2018, all in electrical engineering. He is currently an Assistant Professor and the Chair of the Department of Electrical Engineering, Jouf University, Saudi Arabia. His research interests include applied RF/radar/EW systems engineering, image processing, signal processing, and artificial intelligence. He was a recipient of several awards from the Bluefield State College and the Saudi Arabian Cultural Mission, USA.

AHSAN ALTAF received the B.Sc. degree (Hons.) in electronics engineering from COMSATS University Islamabad, Pakistan, in 2012, and the Ph.D. degree in electrical engineering from Istanbul Medipol University, Istanbul, Turkey, in 2021. From 2012 to 2015, he was a Laboratory Engineer with the Department of Electrical Engineering, City University of Science and Information Technology, Pakistan. From 2015 to 2021, he was a Graduate Research Assistant with Istanbul Medipol University. His research interests include MIMO antenna systems, RF/microwave devices, scattering of electromagnetic waves, and computational electromagnetics. He was a recipient of the Institute's Gold Medal from COMSATS University Islamabad.

TANVEERUL HAQ (Member, IEEE) was born in Multan, Pakistan, in January 1988. He received the B.S. degree in electrical engineering from Bahauddin Zakariya University, in 2011, the M.S. degree in electronic engineering from the Ghulam Ishaq Khan Institute of Engineering Sciences and Technology, in 2014, and the Ph.D. degree from the School of Electronic and Information Engineering, Beihang University, Beijing, China. In 2015, he joined the School of Electrical Engineering, The University of Faisalabad, as a Lecturer. He is currently working as a Chief Executive Officer and a Senior Researcher with the INZA Research Laboratory for Electromagnetic Field and Microwave Engineering. His research interest includes complementary metamaterial based microwave and THz devices with potential application in the electronics and biomedical sector.